Thermoelectric power of doped BSCCO superconductors and marginal Fermi liquid theory

1993 J. Phys.: Condens. Matter 5 669

(http://iopscience.iop.org/0953-8984/5/6/004)

J. Phys.: Condens. Matter 5 (1993) 669–678. Printed in the UK

Thermoelectric power of doped BSCCO superconductors and marginal Fermi liquid theory

Renuka Rajput†, Deepak Kumar†, R G Sharma‡ and Y S Reddy‡
† School of Physical Sciences, Jawaharlal Nehru University, New Delhi-110067, India
‡ National Physical Laboratory, New Delhi-110012, India

Received 26 August 1992, in final form 13 November 1992

Abstract. Measurements of thermoelectric power of BSCCO superconductors doped with Sb and Li at various concentrations are reported. We also report a calculation of thermoelectric power based on the marginal Fermi liquid hypothesis. The calculation is valid above the transition temperature in the temperature range where the superconducting fluctuations play no significant role. The measured TEP data fit the derived formula rather well in the above temperature range (which in this case is 130 K to 300 K). Using the fits, the basic parameters—such as Fermi energy and those involved in the marginal Fermi liquid hypothesis—are derived.

1. Introduction

The thermoelectric power (TEP) of high-T_c superconductors has been extensively studied in the last few years [1–13]. Although initially a lot of variation was observed in the thermopower data, some clear trends regarding magnitude, sign and temperature variation for a number of high-T_c compounds are now discernible. These trends pose a great theoretical challenge, as the TEP exhibits rather large departure, as do other normal-state transport properties, from expectations based on the simple Mott formula, which along with basic expressions for the phonon-drag contribution suffices for at least qualitative understanding of the TEP of simple metals. As examples of TEP anomalies observed in high-T_c materials, we mention the following which we believe are the major ones.

(i) For a number of classes of materials, the TEP has a positive sign, but at the same time its temperature variation has a negative slope. This is quite contrary to Mott's formula according to which the sign and slope of the TEP should be the same.

(ii) Linear extrapolation of the high-temperature TEP gives a large zero-temperature intercept, which is again contrary to the expectation that the TEP must be zero at zero temperature.

(iii) The TEP exhibits a broad precursor peak just above the transition temperature before becoming zero at the transition temperature itself.

Since at present we do not have a clear theoretical understanding of even the simplest transport property, such as resistance, it is not surprising that not much effort has been reported regarding the interpretation of TEP data.

One purpose of this paper is to make use of the marginal Fermi liquid (MFL) hypothesis [14] to calculate the TEP. The MFL hypothesis is a single statement

0953-8984/93/060669+10$07.50

about the polarizability of the electron system in high-T_c materials, which provides a qualitative explanation for a number of experimental results [14], though the origin of the hypothesis is not quite understood. We find that the use of the MFL hypothesis gives a formula for the TEP which is in good accord with the general trends noted as points (i) and (ii) above. We then attempt to obtain a quantitative comparison of the formula with our TEP measurements on doped Bi systems. We have carried out measurements on $Bi_{1.6}Pb_{(0.4-x)}Sb_xSr_{1.6}Ca_2Cu_3O_y$ with Sb concentration varying between 0.0 and 0.2, and $Bi_{1.6}Pb_{(0.4-x)}Li_xSr_{1.6}Ca_2Cu_3O_y$ with Li concentration varying between 0.0 and 0.3. Rather good fits are obtained assuming reasonable values of parameters such as effective carrier mass and carrier density. This also enables us to discuss the values of some parameters contained in the MFL hypothesis. Encouraged by these rather nice fits to our data, we have also fitted the formula with success to some other data reported in the literature. Point (iii) in the above discussion is believed to be related to two-dimensional superconducting fluctuations, which we will discuss elsewhere [15].

2. Theory

The TEP S is composed of two components, namely the diffusion component S_d and the phonon-drag component S_g. According to the elementary theory of degenerate free electron gas [16]

$$S_d = \pi^2 k_B^2 T/2e\epsilon_F \tag{1}$$

and

$$S_g = C_g/3ne \tag{2}$$

where e is the charge of the carrier, ϵ_F the Fermi energy, n the electron density and C_g the lattice specific heat. At low temperatures S_g varies as T^3 and at high temperatures as $1/T$. To incorporate the detailed many-body effects, S is expressed as a ratio of two coefficients obtained from Kubo type correlators [17],

$$S = -(1/T)L_{12}/L_{11} \tag{3}$$

where L_{11} and L_{12} are obtained from the current–current correlators of the following form

$$L_{12}(i\omega_n) = \frac{1}{3i\omega_n \beta\Omega}\int_0^\beta d\tau \exp(i\omega_n\tau)\langle T(j_Q(\tau)\cdot j_e(0))\rangle \tag{4}$$

$$L_{11}(i\omega_n) = \frac{1}{3i\omega_n \beta\Omega}\int_0^\beta d\tau \exp(i\omega_n\tau)\langle T(j_e(\tau)\cdot j_e(0))\rangle \tag{5}$$

where ω_n denotes the Matsubara frequency, Ω denotes volume and j_e and j_Q denote respectively the electric current and heat current operators. The coefficients L_{12} and L_{11} are obtained by the following limiting procedure [17]

$$L = \lim_{\omega\to 0} L(i\omega_n \to \omega + i\delta). \tag{6}$$

Using the standard expression for j_e and an approximate expression for j_Q, given by

$$j_Q = \sum_{ks} \frac{\hbar k}{m}(\epsilon_k - \epsilon_F) c^\dagger_{ks} c_{ks} \tag{7}$$

one arrives at the following expression [17]

$$L_{11} = \frac{2\hbar^2 e^2}{3m^{*2}} \frac{1}{\Omega} \sum_k k^2 \int \frac{d\epsilon}{2\pi} \left(-\frac{dn_F(\epsilon)}{d\epsilon}\right) G_r(k,\epsilon) G_a(k,\epsilon) \gamma(k, \epsilon - i\delta, \epsilon + i\delta) \tag{8}$$

$$L_{12} = \frac{2\hbar^2 e^2}{3m^{*2}} \frac{1}{\Omega} \sum_k k^2 (\epsilon_k - \epsilon_F) \int \frac{d\epsilon}{2\pi} \left(-\frac{dn_F(\epsilon)}{d\epsilon}\right) G_r(k,\epsilon) G_a(k,\epsilon) \gamma(k, \epsilon - i\delta, \epsilon + i\delta) \tag{9}$$

where $n_F(\epsilon)$ is the Fermi function, G_r and G_a are retarded and advanced single-particle propagators, γ is related to the vertex function and m^* is the effective mass of the carrier. At this point, we make use of the single-particle self-energy $\Sigma(k,\epsilon)$ proposed in the MFL hypothesis [14]

$$\Sigma(k,\epsilon) = \lambda[\epsilon \ln(x/\hbar\omega_c) - i(\pi/2)x] \tag{10a}$$

$$x = \max(|\epsilon|, ak_BT) \tag{10b}$$

where λ is a dimensionless coupling constant, a is a constant of the order of 2 and $\hbar\omega_c$ is a cut-off frequency such that the above expression is valid only for $\epsilon < \hbar\omega_c$. Writing $\Sigma(\epsilon) = \Sigma_R(\epsilon) - i\Gamma(\epsilon)$, and performing sums over k, one finds

$$L_{11} = \frac{ne^2}{m^*} \int \frac{d\epsilon}{2\pi} \left(-\frac{dn_F(\epsilon)}{d\epsilon}\right) \frac{\gamma(k_F, \epsilon - i\delta, \epsilon + i\delta)}{2\Gamma(\epsilon)} \tag{11}$$

and

$$L_{12} = \frac{ne}{m^*} \int \frac{d\epsilon}{2\pi} \left(-\frac{dn_F(\epsilon)}{d\epsilon}\right) Q(\epsilon) \tag{12}$$

where with usual approximations

$$Q(\epsilon) = \left\{1 + \frac{\epsilon - \Sigma_R(\epsilon)}{\epsilon_F}\right\}^{3/2} (\epsilon - \Sigma_R) \frac{\gamma(k_F, \epsilon - i\delta, \epsilon + i\delta)}{2\Gamma(\epsilon)}. \tag{13}$$

Note that in deriving $Q(\epsilon)$, asymmetry of the density of states around the Fermi level is crucial. On neglecting vertex corrections, i.e. setting $\gamma = 1$, and evaluating integrals over ϵ in the degeneracy limit, we find

$$L_{11} = ne^2\hbar/m^*\pi\lambda k_BT \tag{14}$$

and

$$L_{12} = (ne\pi^2 k_B^2 T^2/2m^*\epsilon_F)[1 - \lambda \ln(ak_BT/\hbar\omega_c)]^2/2\Gamma(0). \tag{15}$$

Note that L_{11} is the same as the conductivity σ. Equations (14) and (15) then lead to the following formula for S_d:

$$S_d = (\pi^2/2)(k_B/e)(k_BT/\epsilon_F)[1 - \lambda \ln(ak_BT/\hbar\omega_c)]^2. \tag{16}$$

Equation (16) is only the diffusive part of the TEP. If we take the Debye temperature of the material to be 400 K, for the temperature range of interest we can use the high-temperature form of the phonon-drag term, to incorporate it as

$$S = S_d + B/T \tag{17}$$

where B is to be determined empirically. Note that unlike other formulae [18, 19] for the high-temperature behaviour of S_d, equation (16) has the correct behaviour in the $T \to 0$ limit.

3. Experimental results

Samples are prepared by the usual solid-state reaction technique in two batches for Sb- and Li-doped specimens. For the Sb-doped specimens, powders of Bi_2O_3, PbO, Sb_2O_5, $SrCO_3$, $CaCO_3$ and CuO were taken in the molar ratio of Bi:Pb:Sb:Sr:Ca:Cu $= 1.6:(0.4-x):x:1.6:2:3$, where x varies from 0 to 0.2. Powders were mixed thoroughly with a pestle and mortar, calcined at 840 °C for 72 h and furnace cooled to room temperature. The calcined powder was again ground, pelletized in the form of rectangular bars, sintered at 850 °C for 72 h and furnace cooled to room temperature.

For specimens doped with Li, powders of Bi_2O_3, PbO, Li_2CO_3, $SrCO_3$, $CaCO_3$ and CuO were taken in the molar ratio of Bi:Pb:Li:Sr:Ca:Cu: $= 1.6:(0.4-x):x:1.6:2:3$ (all 99.99% pure). These powders were mixed thoroughly and calcined at 820 °C for 140 h. The calcined powder was ground and pressed in the form of rectangular bars ($45 \times 4 \times 3$ mm^3), these bars were sintered at 840 °C for 72 h. A final sintering was carried out at 845 °C for 72 h.

The samples were characterized by the x-ray diffraction technique. Room temperature XRD patterns were recorded for the specimens in a 2θ range of 3° to 45° using Cu Kα radiation. For all the specimens, electrical resistance and thermopower were measured. Resistance was measured using the four-probe technique, while the TEP was measured using a differential method [13] in the temperature range from 80 K to 300 K. The TEP cryostat has a provision for pumping the liquid nitrogen, so that the TEP can be measured down to temperatures even lower than 80 K.

The transition temperature (T_{c0}) is obtained by following the resistance of the specimens as shown in figure 1. Normalized resistance (R_T/R_{210}) versus temperature curves are plotted for specimens of $Bi_{1.6}Pb_{0.4-x}Sb_xSr_{1.6}Ca_2Cu_3O_y$ with $x = 0$, 0.1 and 0.2. A small concentration (0.1) of Sb increases the T_{c0} to 98 K from 90 K (T_{c0} of specimen without Sb), but further increase in Sb concentration reduces T_{c0} to a large extent ($T_{c0} = 84$ K for $x = 0.2$). The normal-state resistance shows metallic behaviour (dR/dT is positive), but metallicity (dR/dT) decreases with Sb doping. Resistance for all three specimens shows a drop at 110 K and finally becomes zero at T_{c0} ($\simeq$ 80 K). For specimens with $x = 0$ and 0.1 the resistance shows only one broad drop but for $x = 0.2$ the resistance shows two drops at temperatures 110 K and 100 K. The onset temperature remains unchanged with Sb doping without any sign of a superconducting transition above 110 K.

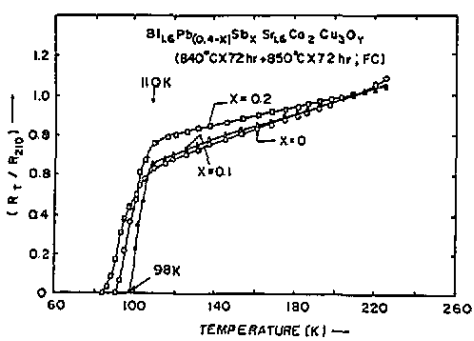

Figure 1. Normalized resistance (R_T/R_{210}) versus temperature plots of $Bi_{1.6}Pb_{(0.4-x)}Sb_xSr_{1.6}Ca_2Cu_3O_y$ specimens for x varying from 0.0 to 0.2.

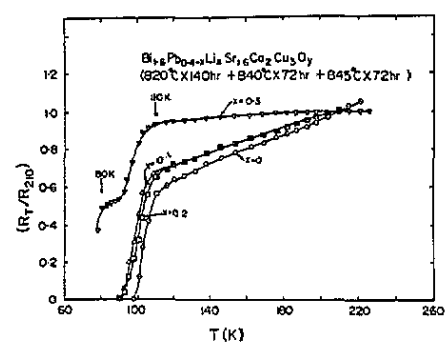

Figure 2. Normalized resistance (R_T/R_{210}) versus temperature plots of $Bi_{1.6}Pb_{(0.4-x)}Li_xSr_{1.6}Ca_2Cu_3O_y$ specimens for x varying from 0.0 to 0.3.

Figure 2 shows the normalized resistance (R_T/R_{210}) versus temperature plots for Li-doped specimens. As is evident from figure 2 the introduction of Li reduces the zero-resistance temperature (T_{c0}) although the onset temperature is the same (110 K) for all the specimens. A small concentration of Li ($x = 0.1$) reduces T_{c0} to 90 K from 98 K (T_{c0} of specimen with $x = 0$). $x = 0.1$ and 0.2 give the same resistance temperature behaviour, whereas $x = 0.3$ shows a two-step resistive transition corresponding to 110 K and 80 K phase transitions with finite resistance down to 78 K. By increasing the Li content the transition width is broadened and metallicity (dR/dT) decreases.

XRD spectra for the Sb-doped specimens show some very interesting results. For the specimen without Sb, the XRD pattern shows only a high-T_c phase with some weak reflections corresponding to Ca_2PbO_4 and Ca_2CuO_4, the contribution from which seems to be very small. With a small addition of Sb, the primary component corresponds to the 2223 phase along with a reflection from the 2201 phase. Apart from the reflections already reported there are some extra peaks corresponding to 2θ values between 29° and 31° with corresponding d values of 2.988, 2.941 and 2.910 Å. These peaks have also been reported by other groups [20, 21]. They have been assigned to a Cu-deficient phase with unit formula $(BiSbPb)_4Sr_4Ca_4Cu_1O_y$. Konstantinov *et al* [20] report this 4441 phase to be monoclinic and non-superconducting above LNT; at the same time Xu *et al* [21] have reported this phase to be responsible for transition temperatures higher than 110 K. Further increase in Sb concentration ($x = 0.2$) shows intense reflections for Ca_2PbO_4, the 2201 phase and the 4441 phase along with the 2223 phase. The intensity of reflections corresponding to the new phase has been increased to a large extent for $x = 0.2$. XRD patterns for all these specimens are shown in figure 3. XRD patterns and R–T curves for these specimens clearly show that Sb neither raises the T_c of the 2223 phase nor gives rise to the formation of any other new phase responsible for a transition temperature higher than 110 K. However, it does lead to the formation of a new Cu-deficient phase, which is either non-superconducting or superconducting with a transition temperature below 110 K. Doping with a small concentration of Sb may stabilize the structure which in turn results in an increase in T_{c0}. The reason for T_{c0} being low (90 K) even for the specimen without Sb may be that the superconducting grains are not well connected, as the specimen preparation lacks the intermediate grinding.

Room temperature XRD spectra for the Li-doped specimens are shown in figure 4. The specimen without Li shows reflections corresponding to the 2223 phase only. Li addition leads to formation of the 2212 phase and the 2201 phase with some other impurities such as Ca_2PbO_4 and CuO. Intensities for these reflections increase with increasing Li content. Appearance of CuO peaks with Li doping is in agreement with the results of Kawai *et al* [22], but they have reported an increase of T_{c0} for the 2212 phase, which is contradictory to our observation of a decrease of T_{c0}. Whether the increase of Li content or the decrease in Pb content results in this kind of behaviour is not very clear from these studies. A Li concentration of 0.3 would correspond to a Pb concentration of 0.1, and that low concentration of Pb itself is responsible for the two-step incomplete transition. An increase in transition temperature, as has been seen in the studies of Kawai *et al* [22] and Matsubara *et al* [23] with the incorporation of Li, is not seen here. Our results suggest that Li does not raise the transition temperature of either phase (2212 or 2223).

The TEP (S) for all the specimens exhibits a similar kind of behaviour and has

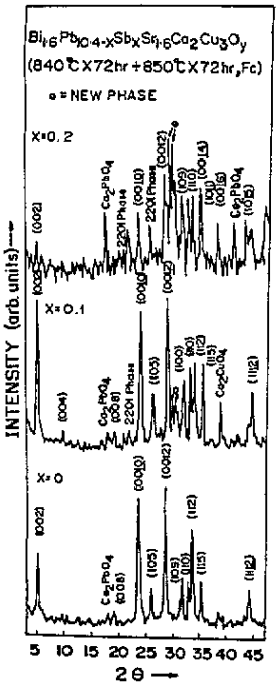

Figure 3. Room temperature XRD patterns for Sb-doped specimens.

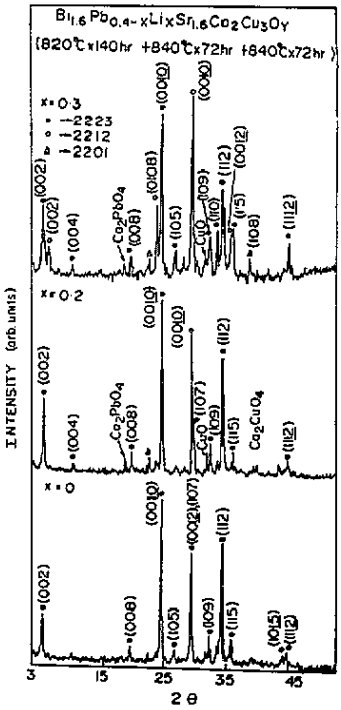

Figure 4. Room temperature XRD patterns for Li-doped specimens.

been plotted against temperature in figures 5 and 6 for Sb-doped and Li-doped specimens respectively. The TEP of all the specimens is positive and decreases with increasing temperature, followed by either a change of sign at higher temperatures or a tendency to change sign. The TEP shows maxima between 120 K and 135 K for all the specimens and the value of this maximum goes down with increasing doping level. The TEP goes to zero at temperature T_{S0}, but this is not the same as the zero-resistance temperature T_{R0}. The maximum value of the TEP (S_m), the temperature corresponding to the maximum in the TEP T_m, the zero-thermopower temperature (T_{S0}) and the zero-resistance temperature T_{R0} are summarized in table 1 for all the specimens.

4. Comparison with theory

In order to compare the experimental TEP data with equation (16), we first make a plot of $(S/T)^{1/2}$ versus $\ln T$, which should be a straight line according to (16). These plots for several systems in the temperature range from 120 K to 300 K are shown in figure 7 and are seen to be good straight lines. These fits are much better than the fits to conventional formulae that we tried (e.g. $S = AT + B/T$). This also means that the phonon-drag term is somehow quite small. We shall discuss this point a little later. In order to achieve quantitative comparisons and obtain values of the parameters involved in the MFL hypothesis, we need to fix some basic parameters. For this, we derive partial information from the conductivity formula, i.e. equation (14),

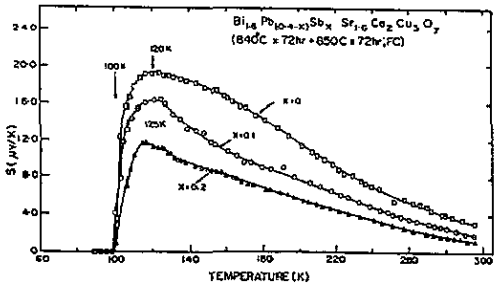

Figure 5. Measured thermoelectric power of the $Bi_{1.6}Pb_{(0.4-x)}Sb_xSr_{1.6}Ca_2Cu_3O_y$ system plotted against temperature for x varying from 0.0 to 0.2.

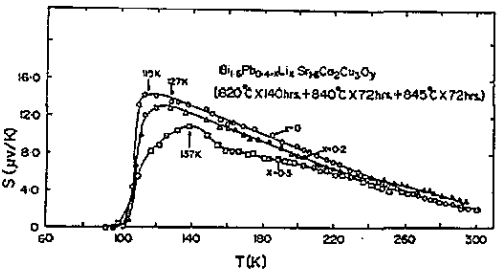

Figure 6. Measured thermoelectric power for the Li-doped system with nominal composition $Bi_{1.6}Pb_{(0.4-x)}Li_xSr_{1.6}Ca_2\ Cu_3O_y$ plotted against temperature for Li concentration varying from 0.0 to 0.3.

Table 1. Values of (a) maximum TEP (S_m), (b) the temperature at which the maximum of the TEP occurs (T_m), (c) the temperature at which the TEP goes to zero (T_{S0}) and (d) the temperature at which the resistance goes to zero (T_{R0}) against the composition of the specimens.

Composition of $Bi_{1.6}Pb_{0.4-x}M_xSr_{1.6}Ca_2Cu_3O_y$	S_m (μV K^{-1})	T_m (K)	T_{S0} (K)	T_{R0} (K)
M = Sb				
$x = 0.0$	19.4	120	98	90
$x = 0.1$	16.4	120	98	98
$x = 0.2$	11.6	115	98	84
M = Li				
$x = 0.0$	14.4	120	101	98
$x = 0.2$	13.0	127	95	90
$x = 0.3$	11.0	137	95	—[a]

[a] Resistance is finite down to 77 K.

which yields the linear slope of resistivity ($d\rho/dT$) to be

$$d\rho/dT = m^*\pi k_B\lambda/ne^2\hbar. \tag{18}$$

Now for our specimens the average value of ($d\rho/dT$) is $1 \times 10^{-7}\Omega$ m K^{-1}. This is also the order of magnitude for other measurements reported in the literature. Note that the slope of the straight line in figure 7 is $-\lambda(\pi^2k_B^2/2e\epsilon_F)^{1/2}$ and its intercept on the vertical axis is $(\pi^2k_B^2/2e\epsilon_F)^{1/2}[1 + \lambda\ln(\hbar\omega_c/ak_B)]$. Thus if we fix n and m^*, we should be able to obtain parameters λ, $\hbar\omega_c$ and ϵ_F. We have taken $n = 3 \times 10^{21}$ cm^{-3} for the pure Bi system, which is roughly the hole density obtained by assuming one hole per unit cell. We take m^* to be five times the electron mass. Equation (17) then yields $\lambda \simeq 4$ (table 2 gives values for all the specimens). Now the slopes and intercepts of straight lines such as that of figure 7 are used to determine ϵ_F and $\hbar\omega_c$. However, these parameters do not enable us to fit the experimental data well. Better fits are obtained for values of ϵ_F and $\hbar\omega_c$ which are about 15 to 25% higher. The simplest way to resolve this discrepancy is to attribute it to the vertex correction factor γ which is present in the formula for conductivity but cancels

out (in this simple theory) from the formula for the TEP. The values of ϵ_F fitting the data best for the TEP are listed in table 2. The values of $\hbar\omega_c$ obtained by a combination of fitting the y-axis intercept in figure 7 and actual fitting with the data are found to be of order 600 K (if we take $a = 2$). These values are much smaller than $\sim$ 3000 K which the authors of the MFL hypothesis expect it to be. This casts some doubt about the consistency of the hypothesis with regard to the TEP, but due to the present lack of understanding of the MFL hypothesis and possible lacunae in the derivation of the TEP formula, it is difficult to comment on this apparent discrepancy. Figure 8 shows some fits to the data obtained by using values of parameters from table 2. Clearly the formula works well for the temperature range from 130 K to 300 K. Above 300 K the predicted curve bends upward after a minimum (at about 380 K in the present instance), whereas the measured TEP in our specimens changes or seems to be changing sign. On the other hand, the TEP data in yttrium and some other rare-earth based compounds do exhibit this trend of turning upwards [3, 11]. Our theory clearly cannot account for a change of sign, which we believe is related to multiband conduction with both electron and hole-type carriers.

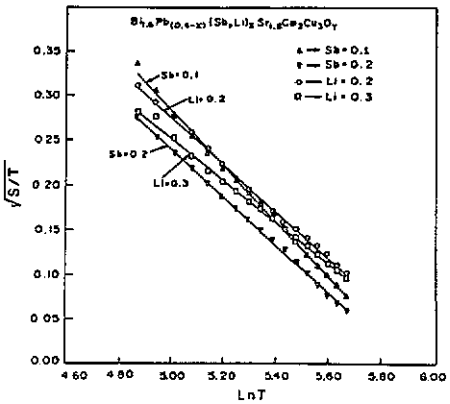

Figure 7. Plots of $(S/T)^{1/2}$ versus $\ln T$ for the Sb- (0.1, 0.2) and Li- (0.2, 0.3) doped specimens in the temperature range 120 K to 300 K.

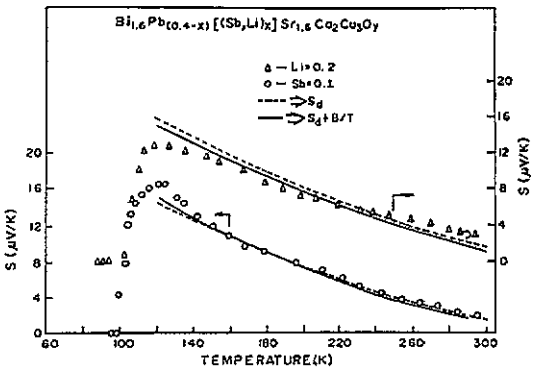

Figure 8. Experimental values of TEP plotted against temperature along with the theoretically calculated values. Dashed lines are plots for the expression of S_d obtained using the marginal Fermi liquid hypothesis, whereas solid lines are for the TEP including the phonon-drag term in S_d.

Next we come to the consideration of the phonon-drag effect. As remarked earlier, equations (16) and (17) suggest a rather small effect. Since the MFL hypothesis implies a lack of well defined quasi-particles, the form of the phonon-drag term may be quite different and its magnitude much smaller than that in a conventional system. In any event, when we fit the data according to (17), we find that reasonably good fits are obtained by taking B to be negative and of the order of 100 to 150 μV. This value of B is one order of magnitude smaller than what would be obtained by conventional fits done according to equations (1) and (2). The values of B are also listed in table 2. Another noteworthy feature of this fit is that the values of the parameters vary rather systematically with dopant concentration. ϵ_F seems to increase linearly with both Li and Sb doping; however, this may not quite reflect the correct situation, as the value

Table 2. Parameters obtained on fitting the experimental data to the TEP formulae given in equations (16) and (17) against the composition of the specimens. Note that two values of ϵ_F are listed, these being obtained by setting $B = 0$ and $B \neq 0$.

Composition of $Bi_{1.6}Pb_{0.4-x}M_xSr_{1.6}Ca_2Cu_3O_y$	λ	ϵ_F (K)	$\hbar\omega_c$ (K)	B (μV K^{-1})	ϵ_F (K)
M = Sb					
$x = 0.0$	4	51 000	600	−150	48 000
$x = 0.1$	4	78 000	600	−140	72 000
$x = 0.2$	4	99 000	600	−120	91 000
M = Li					
$x = 0.0$	4	65 000	600	−100	60 000
$x = 0.2$	4	70 000	600	−80	70 000
$x = 0.3$	4	90 000	600	−60	80 000
$YBa_2Cu_3O_{7-\delta}$ [11]					
$\delta = 0.12$	1	220 000	600	−50	160 000
$\delta = 0.02$	2	220 000	600	50	240 000

of carrier concentration has been kept fixed throughout these fits. Finally we show the fit of the data of Cohn *et al* [11] to our equations (16) and (17) in figure 9. Again one sees rather good agreement, between temperatures of 130 K and 300 K.

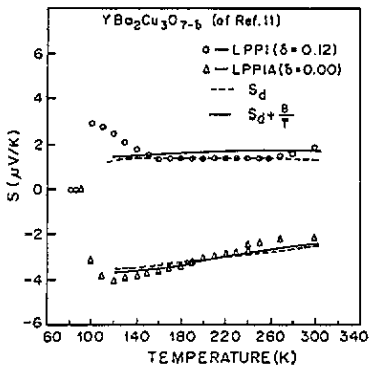

Figure 9. Thermopower data of Cohn *et al* along with theoretically calculated values plotted against temperature.

5. Summary

In conclusion, we would like to point out that measurement of thermopower in Bi superconductors with two dopants shows similar trends in temperature behaviour. These data can be nicely fitted in a temperature range from 130 K to 300 K by a formula derived on the basis of the MFL hypothesis. These fits allow us to make reasonable estimates for the coupling parameter λ and cut-off frequency $\hbar\omega_c$. The value of $\hbar\omega_c \simeq 60$ meV is smaller by a factor of five than the value estimated from other experiments. The values of various parameters listed in table 2 show systematic and expected trends with doping.

Acknowledgment

DK wishes to acknowledge a very useful discussion with Dr C M Varma.

References

[1] Chen J T, McEwan C J, Wenger L E and Logothetis E M 1987 *Phys. Rev.* B **35** 7124
[2] Uher C, Kaiser A B, Gmelin E and Walz L 1987 *Phys. Rev.* B **36** 5676
[3] Srinivasan R, Sankarnarayanan V, Raju N P, Natrajan S, Varadraju U V and Subbarao G V 1987 *Pramana* **29** L225
[4] Lee S C, Lee J H, Suh B J, Moon S H, Lim C J and Khim Z G 1988 *Phys. Rev.* B **37** 2285
[5] Yu R C, Naughton M J, Yan X, Chaikin P M, Holtzberg F, Greene R L, Stuart J and Davies P 1988 *Phys. Rev.* B **37** 7963
[6] Clayhold J, Hagen S, Wang Z Z, Ong N P, Tarascon J M and Barboux P 1989 *Phys. Rev.* B **39** 777
[7] Kang W N, Cho K C, Kim Y M and Choi Mu-Yong 1989 *Phys. Rev.* B **39** 2763
[8] Forro L, Raki M, Henry J H and Ayache C 1989 *Solid State Commun.* **69** 1097
[9] Ouseph P J and O'Bryan M R 1990 *Phys. Rev.* B **41** 4123
[10] Devaux F, Manthiram A and Goodenough J B 1990 *Phys. Rev.* B **41** 8723
[11] Cohn J L, Wolf S A, Selvamanicham V and Salama K 1990 *Phys. Rev. Lett.* **66** 1098
[12] Kaiser A B and Uher C 1991 *Studies of High Temperature Superconductors* vol 7, ed A V Narlikar p 353
(This is a review on thermopower in which reference to other work can be found)
[13] Jha S R, Rajput R, Kumar D, Reddy Y S and Sharma R G 1992 *Solid State Commun.* **81** 603
[14] Varma C M, Littlewood P B, Schmitt-Rink S, Abrahams E and Ruckenstein A 1989 *Phys. Rev. Lett.* **63** 1996
Varma C M 1989 *Int. J. Mod. Phys.* B **3** 2083
[15] Kumar D to be published
[16] MacDonald D K C 1962 *Thermoelectricity* (New York: Wiley)
[17] Mahan G D 1981 *Many-Particle Physics* (New York: Plenum)
[18] Kwak J F and Beni G 1976 *Phys. Rev.* B **13** 652
[19] Rao C N R, Ramakrishnan T V and Kumar N 1990 *Physica* C **165** 183
[20] Konstantinov K, Karbanov S and Vassilev V 1990 *Z. Phys.* B **81** 151
[21] Xu Q, Cheng T, Li X-G, Yang L, Fan C, Wang H, Mao Z, Peng D, Chen Z and Zhang Y 1990 *Supercond. Sci. Technol.* **3** 373
[22] Kawai T, Horiuchi T, Mitsui K, Ogura K, Takagi S and Kawai S 1989 *Physica* C **161** 561
[23] Matsubara I, Tonigawa H, Ogura T, Yamashita I, Kinoshita M and Kawai T 1990 *Physica* C **167** 503